IL NUOVO CIMENTO VOL. 33 A, N. 2 21 Maggio 1976

Thermal Excitation of Nucleons in Relativistic High-Density Nuclear Shock Waves (*).

J. HOFMANN, W. SCHEID and W. GREINER

Institut für Theoretische Physik der Johann Wolfgang Goethe Universität Frankfurt am Main, Germany

(ricevuto il 26 Gennaio 1976)

Summary. — The possibility of excitation of nucleonic resonances in relativistic heavy-ion collisions is investigated. The high-density nuclear shock waves are treated in a relativistic hydrodynamical model.

1. – Introduction.

The possibility of propagation of density waves through nuclear matter was suggested in early papers [1-5]. One has to distinguish, however, the propagation of sound waves with *small* density amplitudes, which travel with sound velocity, and which are considered in ref. [1], from shock waves with *high*-density amplitudes, for which the rest density in the shock zone is large compared to the equilibrium density [2]. The latter waves are denoted as « high-density nuclear shock waves » (HDNSW). These high-density waves [2] are of great fundamental importance, because they furnish the key mechanism

(*) Supported by Bundesministerium für Forschung und Technologie and by the Gesellschaft für Schwerionenforschung (GSI).

(1) A. E. GLASSGOLD, W. HECKROTTE and K. M. WATSON: *Ann. of Phys.*, **6**, 1 (1959).

(2) W. SCHEID, H. MÜLLER and W. GREINER: *Phys. Rev. Lett.*, **32**, 741 (1974).

(3) W. SCHEID, J. HOFMANN and W. GREINER: *Proceedings of the Symposium on Physics with Relativistic Heavy Ions at LBL* (Berkeley, Cal., 1974).

(4) G. F. CHAPLINE, M. H. JOHNSON, E. TELLER and M. S. WEISS: *Phys. Rev. D*, **8**, 4302 (1973).

(5) C. Y. WONG and T. A. WELTON: *Proceedings of the International Conference on Reactions between Complex Nuclei*, Vol. **1** (Amsterdam, 1974); *Phys. Lett.*, **49** B, 243 (1974).

for producing high nuclear densities ($\varrho^0/\varrho_0^0 \geqslant 2$), which are in turn important to study the behaviour of nuclear matter under strong compressions (compressibility, density isomers, pion condensation, σ-condensation, etc.). Furthermore it has been shown in ref. [6] that only HDNSW describe the measured angular distributions of Mach-shock particle emission in high-energy nucleus-nucleus collisions.

The aim of this paper is the generalization of the nonrelativistic model of ref. [2] to relativity, the inclusion of nucleon resonances (which we call thermal pionization [3]), and the study of their influence on the angular distribution of Mach-shock particles ejected in high-energy heavy-ion collisions.

The validity of hydrodynamics was extensively discussed in previous papers [1-7]. Even though the longitudinal-momentum decay length [7] raises at laboratory energies above 700 MeV/N, shock waves will also occur above this energy, because of thermal excitation of nucleons into nucleonic resonances, pion production [4] and pion condensation phenomena [8] reducing the mean free path appreciably. Even though the hydrodynamical picture and concepts are used in our investigations, it should be clearly kept in mind, that they are limited for describing all the variety of new phenomena encountered in a relativistic nucleus-nucleus collision. A model description is therefore appropriate, especially because it allows to formulate the nonstandard hydrodynamical effects (pionization, crystallization of matter in phase transitions to density isomers) in a simple and clear way.

2. – The model.

In order to learn the essential features of a relativistic compression process, we restrict ourselves to relativistic central collisions of two identical nuclei whose volumes are divided into three parts, namely an ellipsoid with axes $a(t)$, $b(t)$ sandwiched between two cut-off spheres with radius R which are relativistically contracted. The relative coordinate between the centres of these spheres is $r(t)$. The problem is treated in the centre-of-momentum system (c.m. system). In this system the cut-off spheres will move unperturbed with constant velocity $\pm v_0$. They have the nuclear equilibrium density ϱ_0^0 which is seen from the c.m. system as $\varrho_0 = \gamma_0 \varrho_0^0$ with $\gamma_0 = 1/\sqrt{1 - v_0^2/c^2}$. Choosing $R = \text{const}$, during the collision, we are dealing with three degrees of freedom, namely a, b, r (fig. 1). Nonrelativistic calculations [3] show that the velocity

---

[6] H. G. BAUMGARDT, J. U. SCHOTT, Y. SAKAMOTO, E. SCHOPPER, H. STÖCKER, J. HOFMANN, W. SCHEID and W. GREINER: *Zeits. Phys.*, **237** A, 359 (1975).

[7] M. I. SOBEL, P. J. SIEMENS, J. P. BONDORF and H. A. BETHE: *Nucl. Phys.*, **251** A, 502 (1975).

[8] V. RUCK, M. GYULASSY and W. GREINER: October 1975, to be published in *Zeits. Phys.*

$\dot{r}$ turns out to be practically time independent. Hence we choose $\dot{r} = 2v_0/(1 + v_0^2/c^2) = \text{const}$, *i.e.* we are concerned with the time dependence of a and b.

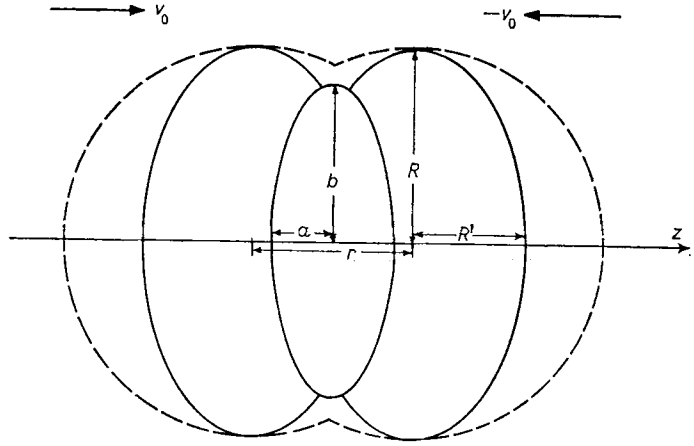

Fig. 1. – The basic features of the relativistic model are shown as seen in the c.m. system. The compression ellipsoid with semi-axes a and b is sandwiched by the ellipsoids which are spheres with radius R in their own rest systems (dashed curves). Their relative distance is denoted by r. As the two ellipsoids move with velocity $v_0, -v_0$, respectively, their radius is relativistically contracted to $R' = \sqrt{1 - (v_0^2/c^2)}\,R$.

The exact solution of the full hydrodynamical problem is very complicated [9] Our model is more feasible and lucid than the full-scale numerical computer solution, and it contains the essential physical features in a transparent way.

3. – Many-phase hydrodynamics for hadronic matter.

To study the formation of nucleonic resonances in the dense, hot matter region, *i.e.* in the compression ellipsoid, and its interplay with the intensity of the shock waves, we consider a thermodynamical theory of nucleons and their excited states. The total rest density of all isobars is denoted by ϱ^0, that of the unexcited nucleons by ϱ_1^0 and the densities of the nucleons in excited isobaric states i shall be ϱ_i^0. If we are concerned with n isobaric states, the relation holds

$$\varrho^0 = \sum_{i=1}^{n} \varrho_i^0 \,. \tag{1}$$

Quantitative results—as presented in the following—indicate that during the collision nuclear matter will be strongly compressed for a time of $2 \cdot 10^{-23}$ s.

---

[9] A. A. Amsden, G. F. Bertsch, F. H. Harlow and J. R. Nix: *Phys. Rev. Lett.*, **35**, 905 (1975).

On the other hand, the cross-section for meson production at relevant energies is of the order of $(10 \div 30)$ mb. If we take $\varrho^0 \approx 3\varrho_0^0$ the equilibration time for the excitation of mesonic degrees of freedom in the shock zone is of the order of $6 \cdot 10^{-24}$ s (ref. [4]). This enables us to use equilibrium thermodynamics [4] as a first approximation. Therefore—within the validity of this model—the densities of the excited states (resonances) are given by the Boltzmann distribution law

$$\varrho_i^0 = \tau_i \varrho_1^0 \exp\left[-\frac{E_i}{T}\right], \tag{2}$$

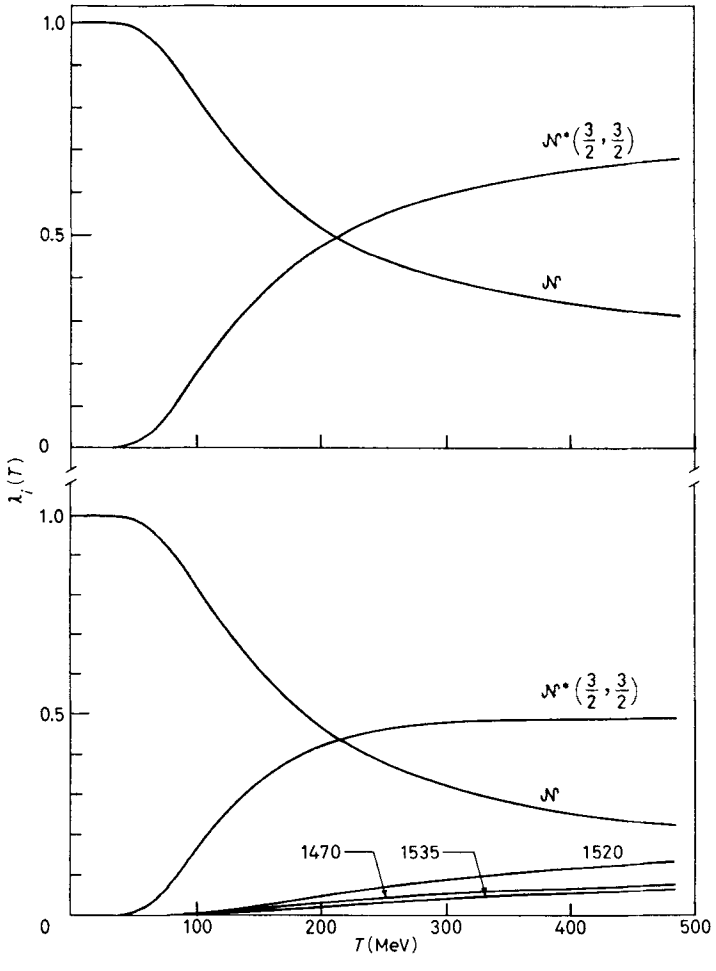

Fig. 2. – The temperature dependence of the occupation numbers λ_i is depicted for nucleons and $\mathcal{N}^*(\frac{3}{2},\frac{3}{2})$-resonances and for nucleons and resonances with $Mc^2 < 1600$ MeV, respectively [10]. The $\mathcal{N}^*(\frac{3}{2},\frac{3}{2})$-state is predominantly occupied.

[10] *Tables of Particle Properties* (Genève, 1974).

where $E_i = (M_{\mathrm{res}_i} - M_0)c^2$ are the excitation energies of the isobaric resonances and T is the temperature of the isobaric gas.

The factor τ_i describes the different occupation probabilities of the excited states i connected with spin and isospin

$$\tau_i = \frac{(2S_{\mathrm{res}_i} + 1)(2I_{\mathrm{res}_i} + 1)}{4} . \tag{3}$$

By (1) we get

$$\varrho_i^0 = \frac{\tau_i \exp[-E_i/T]}{\sum_{k=1}^{n} \tau_k \exp[-E_k/T]} \varrho^0 \equiv \lambda_i(T)\varrho^0 . \tag{4}$$

The temperature dependence of $\lambda_i(T)$ (fig. 2) shows that at $T \approx 200$ MeV about 50 % of baryonic matter is isobaric.

4. – Ansatz for the energy of the model.

The total energy E is given by

$$E = \int \gamma W(\varrho^0, T)\, \varrho \, \mathrm{d}V . \tag{5}$$

Here ϱ denotes the densities in the individual regions: $\varrho = \varrho_0$ in the cut-off spheres and $\varrho > \varrho_0$ in the ellipsoidal region. The velocity field enters the total energy (5) by the factor $\gamma = 1/\sqrt{1 - v^2/c^2}$. The energy per particle $W(\varrho^0, T)$ is measured in its rest frame, depending on the rest density ϱ^0 and temperature T and has the following structure:

$$W(\varrho^0, T) = M_0 c^2 + B_0 + E_{\mathrm{comp}} + E_{\mathrm{therm}} + E_{\mathrm{res}} . \tag{6}$$

Here we denote the nucleon mass $M_0 c^2 \approx 939$ MeV, the binding energy of unexcited ground-state matter $B_0 \approx -16$ MeV, the thermal energy E_{therm} and the energy of the resonance excitation E_{res}. For the compression energy we use the simplified ansatz

$$E_{\mathrm{comp}} = \frac{C}{2\varrho^0 \varrho_0^0} (\varrho^0 - \varrho_0^0)^2 , \tag{7}$$

which is quadratic in the deviation of the rest density ϱ^0 from the equilibrium value $\varrho_0^0 \approx 0.17$ fm^{-3}. The constant C is related to the compression constant K of nuclear ground-state matter

$$K = 9C = 9\varrho_0^{02} \frac{\partial^2 W(\varrho^0, T = 0)}{\partial \varrho^{02}} \bigg|_{\varrho^0 = \varrho_0^0} . \tag{8}$$

The compression term depends on the total density, *i.e.* it is assumed to be the same for all isobaric resonances, and contains approximatively the mutual interactions between them. For the thermal energy per baryon we use an ansatz quadratic in the temperature representing a Fermi gas

$$E_{\text{therm}} = \tfrac{1}{2} T^2 \varrho^{0-\frac{1}{3}} \sum_{i=1}^{n} \beta_i \lambda_i^{-\frac{1}{3}}, \tag{9}$$

with the statistical weight factors

$$\beta_i = \left(\frac{2\tau_i \pi}{3}\right)^{\frac{1}{3}} \frac{M_i c^2}{(\hbar c)^2}. \tag{10}$$

These all are simplifying approximations to the isobaric gas. We accept them presently, because of the limited knowledge about the isobaric gas. Obviously the resonance excitation energy is

$$E_{\text{res}} = \sum_{i=1}^{n} E_i \lambda_i(T) \tag{11}$$

with λ_i defined in eq. (4).

Figure 3 shows $(W(\varrho^0, T) - M_0 c^2)$ for different values of T. Obviously the minimum of nuclear matter shifts with temperature towards higher densities,

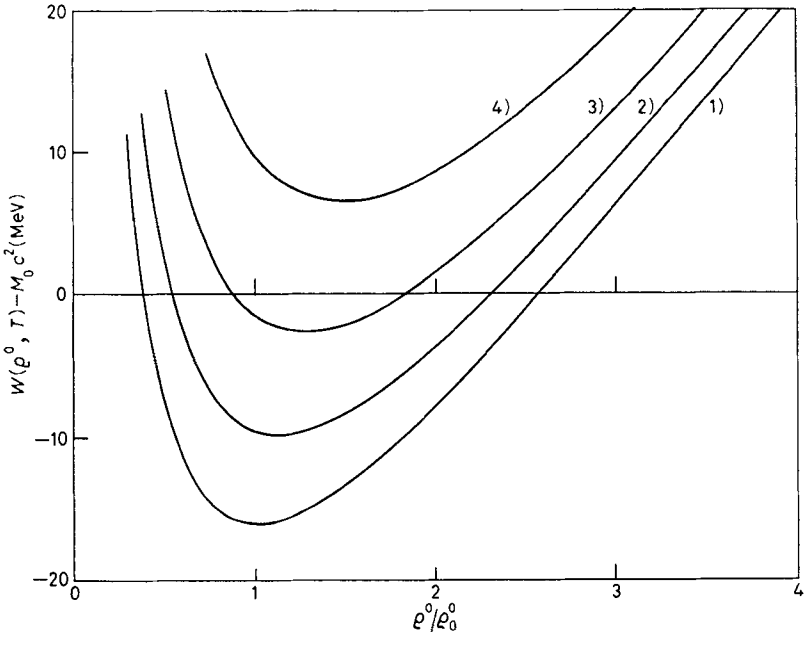

Fig. 3. – The energy density functional in infinite nuclear matter is shown for temperatures of $T = 0$ MeV to $T = 20$ MeV. The Fermi-gas model of nuclear matter is used to calculate the thermal energy. The compression constant is $K = 300$ MeV. The shift of the minimum is a result of the additional thermal energy. 1) $T = 0$ MeV, 2) $T = 10$ MeV, 3) $T = 15$ MeV, 4) $T = 20$ MeV.

which is plausible. To calculate the energy as function of the geometrical co-ordinates a, b and r and their velocities, we make the following assumptions about the density distribution, and the velocity field (fig. 4): The rest density in the cut-off spheres is the equilibrium density ϱ_0^0. The density in the ellipsoid is assumed to be homogeneous. Its value can be calculated using baryon conservation as

$$\varrho = \frac{2R^3 - (3/2\pi)\gamma_0 V_{\text{sph}}}{ab^2}\varrho_0^0 . \tag{12}$$

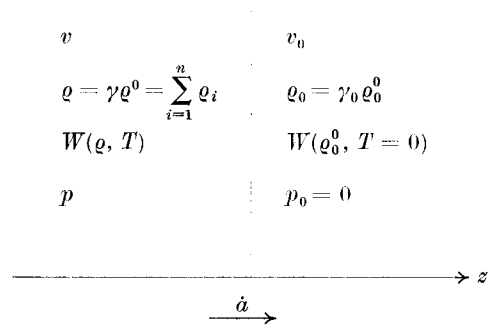

Fig. 4. – The sharp discontinuity, *i.e.* the shock front, is schematically depicted. It separates regions with different velocity fields and variables of state. In the c.m. system the velocity of the shock front is equivalent to the velocity $\dot{a}$ of the geometrical co-ordinate.

Therein the volume of one of the contracted cut-off spheres is given by

$$V_{\text{sph}} = \frac{2}{3}\pi\left[\gamma_0 R^3\left(\frac{1}{\gamma_0} - \alpha\right)^2\left(1 + \frac{\gamma_0}{2}\alpha\right) - ab^2(1-\beta)^2\left(1 + \frac{\beta}{2}\right)\right] \tag{13}$$

with $\alpha = (z_0 - r/2)/R$, $\beta = z_0/a$ and

$$z_0 = \frac{\gamma_0^2 r}{2(b^2/a^2 - \gamma_0^2)}\left\{\sqrt{1 + \left(\frac{b^2}{a^2} - \gamma_0^2\right)\left(\frac{1}{\gamma_0^2} + \frac{4(b^2 - R^2)}{\gamma_0^4 r^2}\right)} - 1\right\} . \tag{14}$$

Because ϱ is assumed to be homogeneous, the rest density $\varrho^0 = \varrho/\gamma$ is co-ordinate dependent. The velocity field $\boldsymbol{v}$ for the various isobaric resonances is assumed to be the same as for the nucleons which holds as long as the resonance rest mass $M_i c^2$ is comparable to the nucleon rest mass. In our calculations we take $M_i c^2 \leqslant 1600$ MeV. To avoid extensive numerical difficulties, we disregard also the pionic field in this calculation. Its velocity field would drastically deviate from the nucleonic one. We therefore expect that in our calculation the temperature of the isobaric gas will be overestimated, because the pions stemming from isobar decay will cool the system (runaway pions).

We will see later from our calculations, that these are not very much pions (about 10), but nevertheless their influence on the thermodynamic properties of the excited matter is important. Those pions stemming from pion condensation are of great importance and, in fact, help considerably to initiate the shock wave, as has been pointed out by RUCK, GYULASSY *et al.* [8]. The interplay of the pion condensation gas with the isobaric gas will be discussed in a forthcoming paper.

The velocity field of the isobaric gas is assumed to be homogeneous within the two cut-off spheres, namely equal to the velocity of the respective centres

$$\frac{\dot{r}}{2} = \frac{v_0}{1 + v_0^2/c^2}, \tag{15}$$

where v_0 is related to the energy per nucleon in the c.m. system $E_{\text{c.m.}}$ by

$$\frac{v_0}{c} = \sqrt{1 - \frac{1}{(E_{\text{c.m.}}/M_0 c^2 + 1)^2}}. \tag{16}$$

In the compression ellipsoid an irrotational velocity field is assumed

$$\boldsymbol{v} = \operatorname{grad} \varphi, \tag{17}$$

which has to fulfil the equation of continuity

$$\operatorname{div}(\varrho \boldsymbol{v}) + \frac{\partial \varrho}{\partial t} = 0. \tag{18}$$

Because of the homogeneous density ϱ this can be rewritten as

$$\Delta \varphi = -\frac{1}{\varrho} \frac{\partial \varrho}{\partial t}. \tag{19}$$

If we use the boundary condition $v = \dot{b}$ and $\boldsymbol{v} \cdot \boldsymbol{e}_z = 0$ along the circle $z = 0$, $x^2 + y^2 = b^2$, the solution of (19) is easily obtained as

$$\boldsymbol{v} = \frac{\dot{b}}{b}(x\boldsymbol{e}_x + y\boldsymbol{e}_y) - \left(\frac{1}{\varrho}\frac{\partial \varrho}{\partial t} + 2\frac{\dot{b}}{b}\right) z\boldsymbol{e}_z. \tag{20}$$

With the densities and the velocity field one can now calculate the total energy according to eq. (5)

$$E = E_{\text{sph}} + E_{\text{ell}}, \tag{21}$$

where

$$E_{\text{sph}} = 2\gamma_0^2 \varrho_0^0 (M_0 c^2 + B_0) V_{\text{sph}}$$

and

$$E_{\text{ell}} = (M_0 c^2 + B_0)\, \varrho \int_{\text{ell}} \gamma \, \mathrm{d}V + \varrho \int_{\text{ell}} \gamma (E_{\text{comp}} + E_{\text{therm}} + E_{\text{res}}) \, \mathrm{d}V \,. \tag{22}$$

Since the compression, thermic and resonance energies are depending on the nonhomogeneous rest frame density ϱ^0 in the ellipsoidal region, the integrals over the thermal and resonance energies lead to elliptic integrals. For simplification, we introduce an average rest density $\bar{\varrho}^0$ in the compression zone by

$$\bar{\varrho}^0 = \frac{3}{4\pi a b^2} \int_{\text{ell}} \varrho^0 \, \mathrm{d}V = \frac{3\varrho}{4\pi a b^2} \int_{\text{ell}} \frac{\mathrm{d}V}{\gamma} \,, \tag{23}$$

and obtain

$$E_{\text{ell}} = \varrho \{ M_0 c^2 + B_0 + E_{\text{therm}}(\bar{\varrho}^0) + E_{\text{res}}(\bar{\varrho}^0) \} \int_{\text{ell}} \gamma \, \mathrm{d}V + \varrho \int \gamma E_{\text{comp}} \, \mathrm{d}V \,, \tag{24}$$

for which one finds easily analytic expressions.

5. – The equations of motion.

The idealization of our model is the sharp discontinuity between the compressed and uncompressed region, which we furtheron denote as « shock front » (fig. 4). At this shock front the state variables, *i.e.* the density ϱ^0, the energy W and the pressure p are discontinueous, whereas we require the continuity of baryon flux, momentum flux and energy flux. This results in the relativistic Rankine-Hugoniot equation (RRH-equation)

$$W^2(\varrho^0, T) - W^2(\varrho_0^0, T = 0) + (p - p_0) \left\{ \frac{W(\varrho^0, T)}{\varrho^0} - \frac{W(\varrho_0^0, T = 0)}{\varrho_0^0} \right\} = 0 \,. \tag{25}$$

The pressure p in the ellipsoidal region is given by

$$p = \frac{C}{2\varrho_0^0} (\varrho^{0^2} - \varrho_0^{0^2}) + \frac{1}{3} T \varrho^{0^{\frac{3}{2}}} \int_0^T \sum_{i=1}^{n} \beta_i \lambda_i^{\frac{3}{2}} \, \mathrm{d}T' \,, \tag{26}$$

and in the cut-off spheres $p_0 = 0$. Equation (25) yields a unique connection between the rest density ϱ^0 and the temperature T which has to be solved by iteration. Figure 5 shows this function for two cases, namely without nucleon resonances, and under inclusion of resonances with masses up to 1600 MeV. Earlier nonrelativistic calculations ([3,7]) show a pole in the density excitation function at $\varrho^0/\varrho_0^0 = 4$ for nucleons and at somewhat higher densities if isobaric resonances are included, whereas in the correct relativistic treatment these

poles vanish ([6]). The velocity of the shock front is easily calculated as ([6,11]) (fig. 6)

$$\frac{v_s}{c} = \sqrt{\frac{pW(\varrho^0, T)}{(W(\varrho^0, T)\varrho^0 - W(\varrho_0^0, T=0)\varrho_0^0)(W(\varrho_0^0, T=0)\varrho_0^0 + p)}}. \tag{27}$$

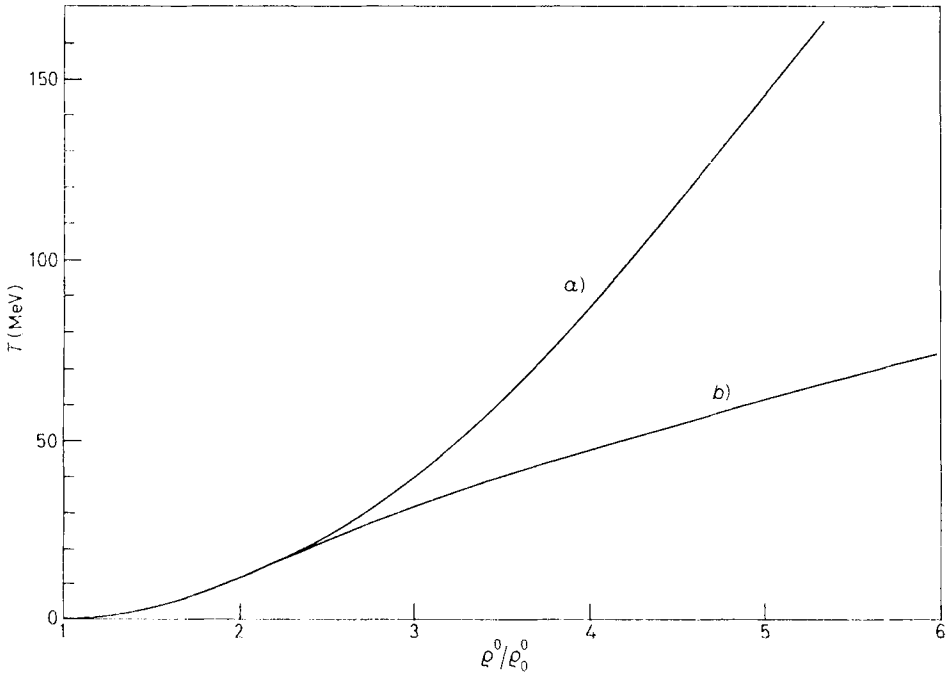

Fig. 5. – The density dependence of the temperature T is shown for $K = 300$ MeV as obtained by the RRH equation. As further calculations show, only few resonances are formed during the collision (about 10), but their influence on the temperature is important. As the resonances cool the nuclear matter to temperatures small compared to the actual Fermi temperature, the quadratic ansatz for the thermal energy (eq. (9)) is justified: *a*) no resonances, *b*) resonances up to 1600 MeV.

Since this relation holds in the rest frame of the unshocked fluid, *i.e.* in one of the cut-off spheres, we have to transform to the ellipsoid moving with v_0 to get the shock velocity as seen from the c.m. system

$$v_s^{\text{c.m.}} = \frac{v_s - v_0}{1 - v_0 v_s/c^2}.$$

([11]) L. D. LANDAU and E. M. LIFSHITZ: *Hydrodynamics* (London, 1958).

In turn $v_s^{\text{c.m.}}$ is identical with the velocity $\dot{a}$ of the ellipsoidal semi-axis

$$\dot{a} = \frac{v_s - v_0}{1 - v_0 v_s/c^2} . \tag{28}$$

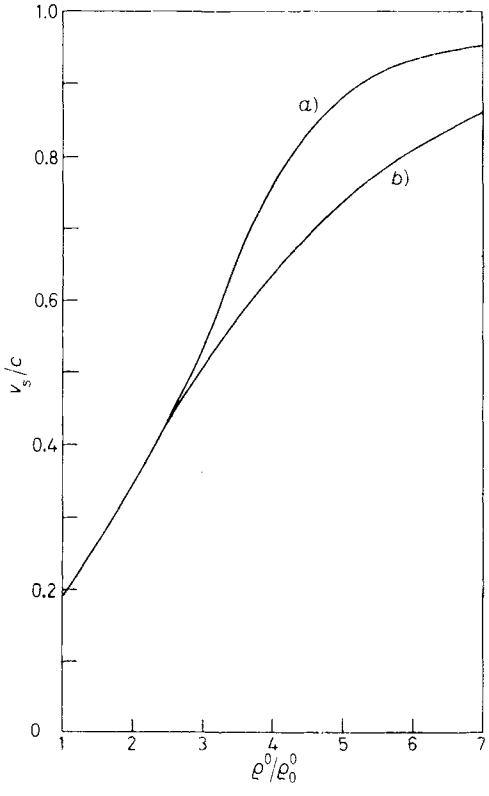

Fig. 6. – The velocity of the shock front v_s/c for $K = 300$ MeV as seen from the laboratory system is shown. v_s/c only in the low-density limit approximates the velocity of sound $c_s/c = 0.18$. For large densities, v_s/c goes to 1. The influence of the resonances is significant: *a*) no resonances, *b*) resonances up to 1600 MeV.

Thus one obtains the two equations

$$F = E - 2A\gamma_0 W(\varrho_0^0, T = 0) = 0 , \tag{29}$$

$$G = \dot{a} - \frac{v_s - v_0}{1 - v_0 v_s/c^2} = 0 , \tag{30}$$

which have to be integrated. Equation (29) expresses energy conservation, while the second one is identically with eq. (28) and gives the connection between the various velocity fields. The two equations are sufficient to obtain the time

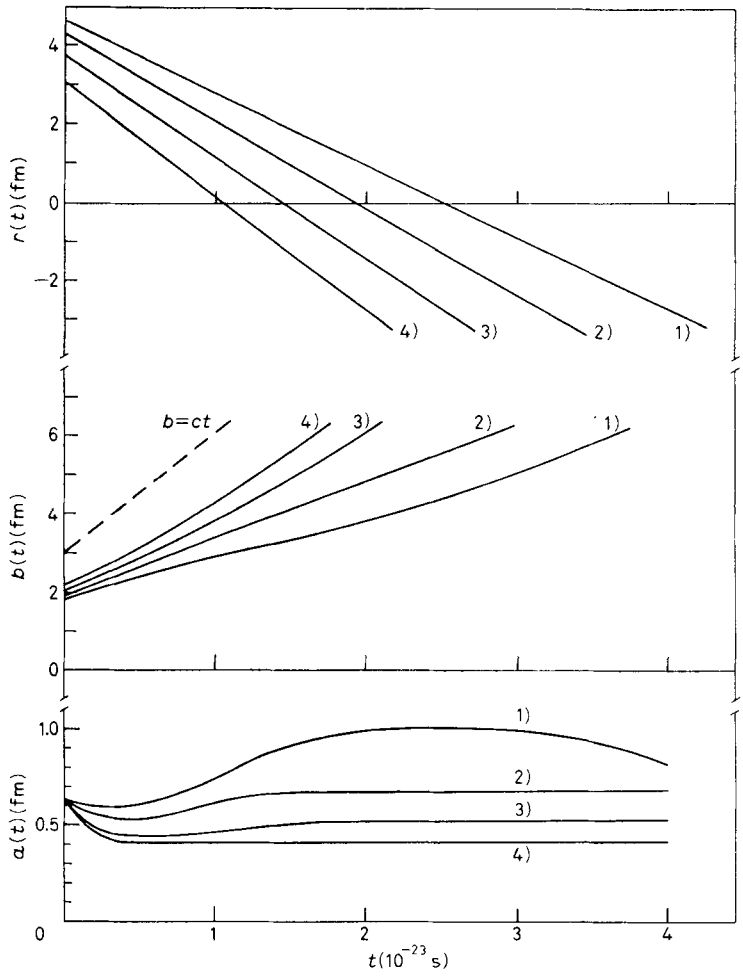

Fig. 7. – The time dependence of the geometrical co-ordinates r, b, a is depicted for laboratory energies per nucleon $E_{lab}/N = 250$ (1)), 500 (2)), 1000 (3)), 2000 MeV (4)) and $K = 300$ MeV. As $\dot{r} = \text{const}$, r is represented by straight lines. For $b(t)$ also the limiting curve $b = ct$ is shown. In contrast to $b(t)$ the co-ordinate $a(t)$ is essentially constant for high energies, which reflects the fact that matter is ejected mainly perpendicularly to the collision axis. Resonances ($Mc^2 < 1600$ MeV).

Fig. 8. – The time dependence of the averaged density as defined in eq. (23) for $K = 300$ MeV and $E_{lab}/N = 250$ (1)), 500 (2)), 1000 (3)), 2000 (4)), 4000 MeV (5)) is shown. At these energies the compression lasts $\approx 5 \cdot 10^{-23}$ s. This justifies the use of equilibrium thermodynamics ([4]). There is *no* limiting density at $\varrho^0/\varrho_0^0 = 4$ as in the nonrelativistic treatment ([3,7]). Resonances ($Mc^2 < 1600$ MeV).

Fig. 9. – The time dependence of the temperature T for $K = 300$ MeV and $E_{lab}/N = 250$ (1)), 500 (2)), 1000 (3)), 2000 MeV (4)) for resonances with $Mc^2 < 1600$ MeV is depicted. The influence of the resonances is evident from the comparison of curve 4) and 5). They resonably lower the temperature in the collision zone. 5) $E_{lab}/N = 200$ MeV, no resonances.

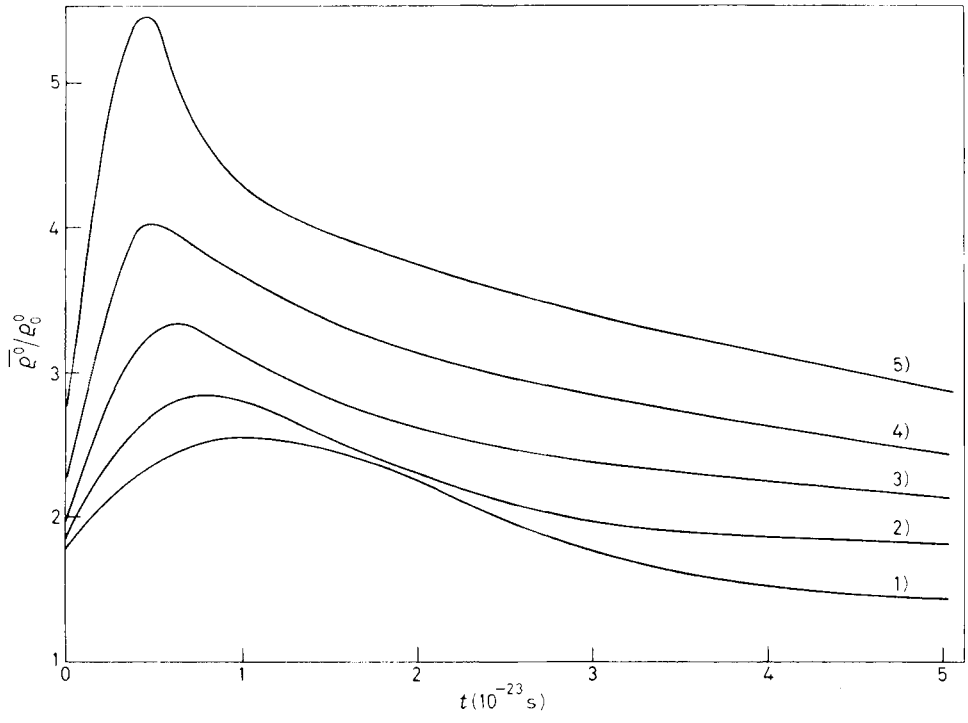

Fig. 8.

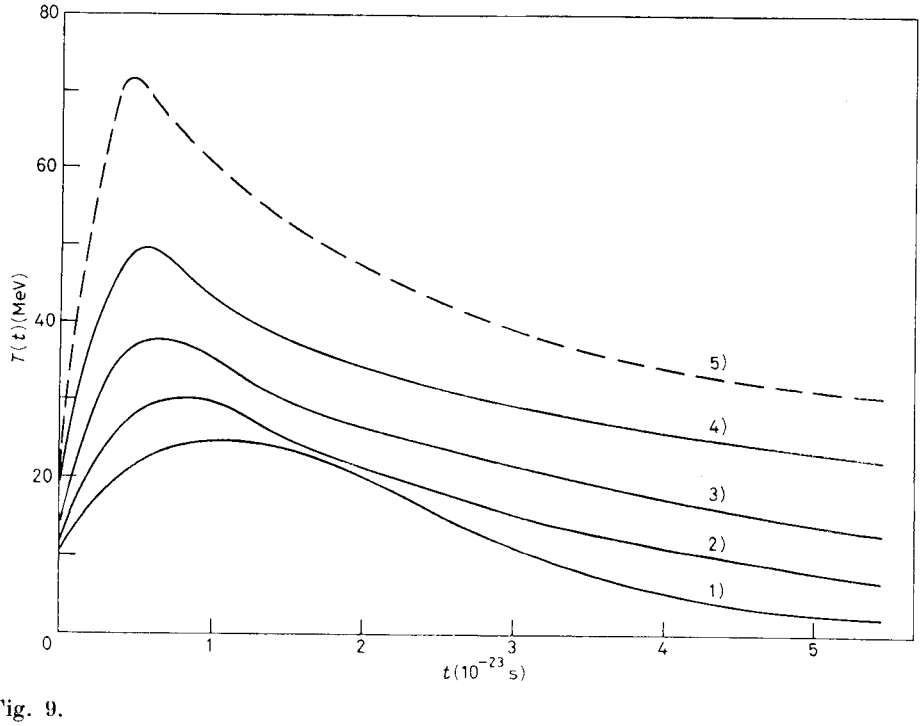

Fig. 9.

dependence of $a(t)$ and $b(t)$. In order to solve these equations for $a(t)$ and $b(t)$ it is advantageous to integrate the following system of first-order differential equations:

$$
(31)\qquad \begin{cases} \dfrac{\partial F}{\partial a}\dot{a} + \dfrac{\partial F}{\partial b}\dot{b} + \dfrac{\partial F}{\partial \dot{a}}\dot{p}_a + \dfrac{\partial F}{\partial \dot{b}}\dot{p}_b = 0\,, \\ \dfrac{\partial G}{\partial a}\dot{a} + \dfrac{\partial G}{\partial b}\dot{b} + \dfrac{\partial G}{\partial \dot{a}}\dot{p}_a + \dfrac{\partial G}{\partial \dot{b}}\dot{p}_b = 0\,, \\ p_a = \dot{a}\,, \qquad p_b = \dot{b}\,. \end{cases}
$$

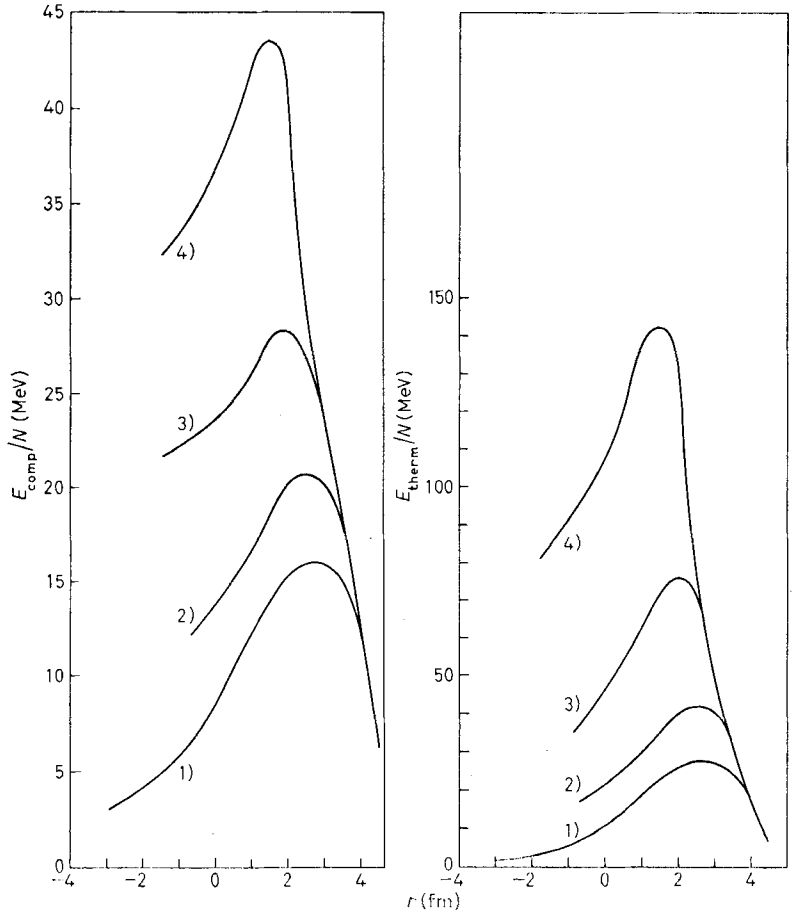

Fig. 10. – The compression and thermal energies per nucleon are shown as function of the relative distance of the two colliding nuclei for $K = 300$ MeV and $E_{lab}/N = 250$ (1)), 500 (2)), 1000 (3)), 2000 MeV (4)). At low laboratory energies compression and thermal energy are of the same magnitude. At high energies E_{therm} is large compared to the compression energy, *i.e.* there is a transition from nuclear matter to a hadronic gas. Resonances ($Mc^2 < 1600$ MeV).

The quantitative results of the numerical integration of the equations of motion (eq. (31)) are depicted in fig. 7, 8 and 9 for laboratory energies per nucleon $E_{lab}/N = \{250, 500, 1000, 2000\}$ MeV and $K = 300$ MeV. Obviously the isobaric matter is predominantly ejected perpendicular to the central collision axis,

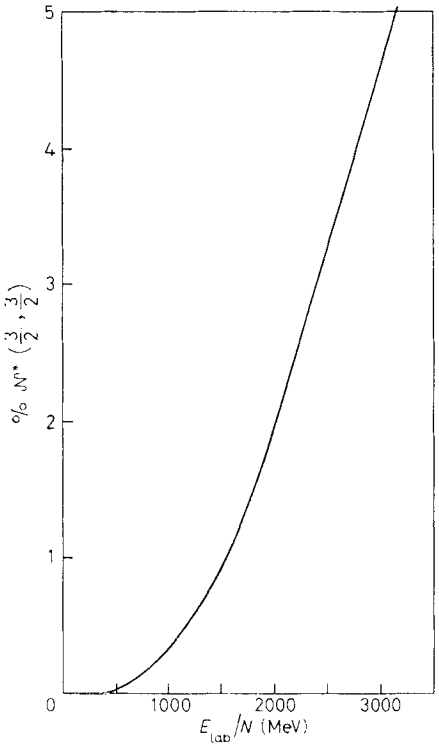

Fig. 11. – The percentage of excited $\mathcal{N}^*(\frac{3}{2}, \frac{3}{2})$ is depicted as function of E_{lab}/N. The curve has been obtained by taking the maximum temperature during the collision and calculating λ (eq. (4)) with it. The higher resonances are excited to a much smaller extent than the $\mathcal{N}^*(\frac{3}{2}, \frac{3}{2})$-resonance. $K = 300$ MeV, resonances ($Mc^2 < 1600$ MeV).

which is infered by the great advance of the semi-axis $b(t)$ with time. Contrary to $b(t)$, the semi-axis $a(t)$ is practically time independent at high collision energies. Figure 10 shows the compression and thermal energies per nucleon in the ellipsoidal region, respectively, for those energies. To estimate the number of thermal pions produced during the collision, we calculated the percentage of excited 1236 MeV resonances as function of the laboratory energy by inserting the maximum temperature reached during the collision into eq. (4) (fig. 11). At energies about 3 GeV/nucleon only about five percent of all nucleons are in the (3, 3)-resonance state.

6. – Application of the model to the interpretation of heavy-ion collision experiments.

Recent experiments ([6]) of bombarding AgCl detectors with α, ^{12}C, ^{16}O at energies between 250 MeV/nucleon and 2.1 GeV/nucleon show significant peaks in the angular distribution. The peak angles shift with increasing energy to lower values. This behaviour can be interpreted as signatures for Mach shock waves of high densities.

If a light nucleus penetrates a larger one, a Mach cone will be formed due to high-density shock travelling to the sides of the projectile, propagating through the target as an energy wave and ejecting particles when it reaches the surface into an angle

$$\cos\varphi = \frac{v_s}{v_{\text{ion}}}, \tag{32}$$

where v_s is the propagation velocity of the shock wave, and v_{ion} the laboratory

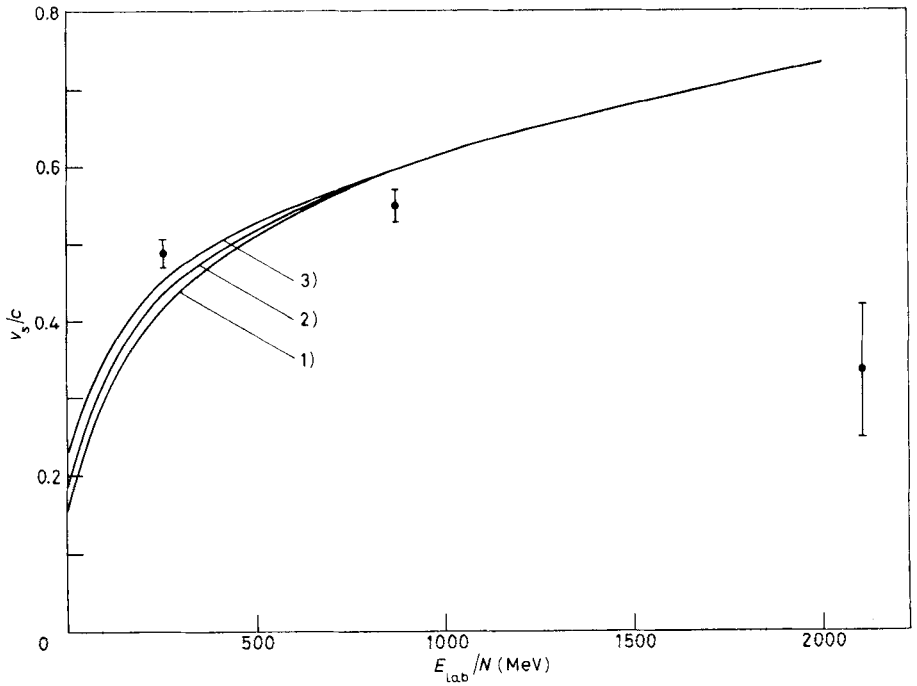

Fig. 12. – v_s/c as function of E_{lab}/N is shown for different compression constants $K = 200$ (1)), 300 (2)), 400 MeV (3)). The theoretical prediction (full curves) is obtained by taking the maximum averaged density $\bar{\varrho}^0_{\max}$ during the collision and inserting it into eq. (27). The experimental values—shown with error bars—are obtained from the experiment ([6]) by the procedure described in the text. Resonances ($Mc^2 < 1600$ MeV).

velocity of the projectile. As φ and v_{ion} are well defined in the experiment, we can determine v_s. We assume that the projectile velocity remains unchanged during the collision. To predict v_s one needs the density in the compression zone (Mach-shock zone). As the model yields an averaged density (fig. 8), it is justified to take the Mach-shock density according to the predictions of the above-described model. Figure 12 shows the velocities $v_s(E_{\text{lab}}/N)$ as obtained from the experiment via the outlined procedure. The theoretical value for it is obtained by calculating within the symmetric collision model the averaged compression density $\bar{\varrho}^0$ and inserting it into eq. (27).

The only free parameter to adjust the theoretical prediction for v_s obtained from the model to the « experimental » value, is the compression constant K. Figure 12 shows v_s^{theo}/c as function of E_{lab}/nucleon for different compression constants $K(200\ \text{MeV} \leqslant K \leqslant 400\ \text{MeV})$.

Obviously at energies $E_{\text{lab}}/N > 1$ GeV the compression constant K has no significant influence on v_s/c, *i.e.* $E_{\text{comp}} \ll E_{\text{therm}}$. This reflects the transition from nuclear matter to a hadronic gas, whose properties are essentially determined by thermodynamics.

At energies $E_{\text{lab}}/\text{nucleon} < 500$ MeV the constant K has only a small influence on v_s/c. The « experimental » value at 250 MeV/nucleon gives $300\ \text{MeV} < K < 500\ \text{MeV}$ as reasonable values. This single data point is not sufficient to give an appreciable value for K. Further experiments in the range of $100\ \text{MeV} \leqslant E_{\text{lab}}/\text{nucleon} \leqslant 500\ \text{MeV}$ are called for.

Moreover we find that the data point at $E_{\text{lab}}/\text{nucleon} = 2100$ MeV is out of range of the theoretical prediction which yields that $v_s/c \to 1$ for $E_{\text{lab}}/\text{nucleon} \to \infty$. From that we conclude that there has to be a special structure in $W(\varrho, T)$ which causes v_s to decrease at $E_{\text{lab}}/\text{nucleon} \approx 2$ GeV. The theoretical implications are discussed in ref. ([12]).

* * *

We thank H. STÖCKER for valuable discussions.

([12]) J. HOFMANN, H. STÖCKER, U. HEINZ, W. SCHEID and W. GREINER: *Phys. Rev. Lett*, **36**, 88 (1976).

● RIASSUNTO (*)

Si studia la possibilità di eccitazione delle risonanze nucleoniche nelle collisioni relativistiche di ioni pesanti. Si trattano le onde d'urto nucleari ad alta densità in un modello relativistico idrodinamico.

(*) *Traduzione a cura della Redazione.*

Тепловое возбуждение нуклонов в релятивистских ядерных ударных волнах с высокой плотностью.

Резюме (*). — Исследуется возможность возбуждения нуклонных резонансов при релятивистских соударениях тяжелых ионов. Ядерные ударные волны с высокой плотностью рассматриваются в релятивистской гидродинамической модели.

(*) *Переведено редакцией.*